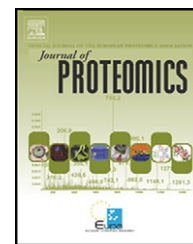


Available online at www.sciencedirect.com

SciVerse ScienceDirect

www.elsevier.com/locate/jprot

Proteomic atlas of the human olfactory bulb

Joaquín Fernández-Irigoyen^a, Fernando J. Corrales^b, Enrique Santamaría^{a,*}

^aProteomics Unit, Biomedical Research Center (CIB), Navarra Health Service, 31008 Pamplona, Spain

^bProteomics Unit, Centre for Applied Medical Research (CIMA), University of Navarra, Pamplona, Spain

ARTICLE INFO

Article history:

Received 12 March 2012

Accepted 7 May 2012

Available online 15 May 2012

Keywords:

Olfactory bulb

Brain

Proteomics

Mass spectrometry

Bioinformatics

ABSTRACT

The olfactory bulb (OB) is the first site for the processing of olfactory information in the brain and its deregulation is associated with neurodegenerative disorders. Although different efforts have been made to characterize the human brain proteome in depth, the protein composition of the human OB remains largely unexplored. We have performed a comprehensive analysis of the human OB proteome employing protein and peptide fractionation methods followed by LC-MS/MS, identifying 1529 protein species, corresponding to 1466 unique proteins, which represents a 7-fold increase in proteome coverage with respect to previous OB proteome descriptions from translational models. Bioinformatic analyses revealed that protein components of the OB participated in a plethora of biological process highlighting hydrolase and phosphatase activities and nucleotide and RNA binding activities. Interestingly, 631 OB proteins identified were not previously described in protein datasets derived from large-scale Human Brain Proteome Project (HBPP) studies. In particular, a subset of these differential proteins was mainly involved in axon guidance, opioid signaling, neurotransmitter receptor binding, and synaptic plasticity. Taken together, these results increase our knowledge about the molecular composition of the human OB and may be useful to understand the molecular basis of the olfactory system and the etiology of its disorders.

© 2012 Elsevier B.V. All rights reserved.

1. Introduction

An indication of the importance of olfactory systems is that ~4% of the genome of many higher eukaryotes is involved in smell function [1]. To cope with the diverse odor molecules, 2% of the mammalian genome is devoted to coding up to 1000 odorant receptors, a large family of G-protein-coupled receptors (GPCRs) that are located on the ciliary membrane surface of olfactory sensory neurons (OSN) in the olfactory epithelium [1,2]. Each OSN expresses only one of the large family of odorant receptors (~1200 and 350 in mouse and humans respectively) [2–4]. The OSNs detect a large variety of odor molecules sending the information through their axons to the OB [5]. The cortical structure of the mammalian OB

contains thousands of signal-processing modules called glomeruli where axons of OSN expressing the same odorant receptor converge into one or two glomeruli, forming excitatory synaptic connections on dendrites of mitral and tufted cells, the output neurons of the OB [5]. The glomerular modules interact with each other through neuronal circuits by local interneurons, periglomerular cells, and granule cells. Periglomerular cells modulate synaptic signaling within the glomerulus as well as between glomeruli contributing to lateral inhibitory/excitatory circuits that regulate the functional specificity in small populations of glomeruli, but their function in odor processing has yet to be fully elucidated [6]. Granule cells are anaxonic and their dendrites form dendrodendritic synapses with the lateral dendrites of 100–150 mitral

Abbreviations: GO, Gene ontology; HBPP, Human Brain Proteome Project; OB, Olfactory bulb; OSN, Olfactory sensory neuron.

* Corresponding author at: Proteomics Unit, Biomedical Research Center, Navarra Health Service, Irunlarrea Street, 31008 Pamplona, Spain. Tel.: +34 848 422 359.

E-mail address: esantamma@navarra.es (E. Santamaría).

1874-3919/\$ – see front matter © 2012 Elsevier B.V. All rights reserved.

doi:10.1016/j.jprot.2012.05.011

or tufted cells and modulate projection neuron output [6]. Interactions between mitral and tufted cells through these interneurons play a central role in the processing of olfactory information [7]. The neuronal circuitry of the OB is highly dynamic, being one of the few structures in the mammalian nervous central system in which there is continued supply of newly generated neurons [8]. This capacity allows ongoing integration of new and different smells [9–11].

In humans, the estimated mean bulb volume is around 35–50 mm³ although the OB size decreases over the course of human adulthood [12,13]. Accumulating evidences confirm that olfactory sensory decline is associated with neurodegenerative disorders including schizophrenia, depression, multiple sclerosis, Huntington's, Alzheimer's and Parkinson's diseases [14–19]. In view of these data, an in depth biochemical characterization of the human OB is mandatory as a first step for understanding smell impairment, gustatory dysfunction, and neurodegenerative disorders including olfactory neuroblastoma.

In the last decade, different proteomic methods have been used to understand the molecular organization and complexity of different regions of the brain [20,21]. Specifically, some carbonylated proteins and fucose α (1–2) galactose glycoproteins have been characterized in mouse OB using targeted-proteomic strategies [22,23]. Moreover, comparative proteomics based on a combination of 2-DE with MS has been used to describe protein profiles of aging olfactory system and proteins linked to olfactory memory in murine OB [24,25]. In particular, proteomic methods have been employed to profile different parts of the olfactory system such as murine olfactory sensory cilia, [26,27] human olfactory cleft mucus, [28] zebrafish OB, [29] and rat OB [30]. However, despite these efforts to identify and catalog the proteins present in the olfactory system of murine models, only a very limited number of proteins have been described in the human OB.

Here we used protein and peptide fractionation strategies coupled to LC-MS/MS to investigate the human OB proteome in depth, and present an extensive analysis of this region of the forebrain. We report the identification of 1529 protein species in OB derived from a single person. We provide a brief overview of molecular functions and subcellular localizations of identified proteins based on GOFact analysis. Extensive database analysis revealed that only 15% of the identified proteins were previously described in the olfactory system and 40% were not previously reported in Human Brain Proteome Project (HBPP) studies. This high-confidence collection of proteins present in human OB may advance knowledge of neurodiseases and aging being useful to elucidate the molecular basis of olfactory system and the etiology of its diseases.

2. Materials and methods

2.1. Sample collection

According to the Spanish Law 14/2007 of Biomedical Research, informed written consent form of the Neurological Tissue Bank of Navarra Health Service was obtained from relatives of a 46-year-old female patient for research purposes. According to

standard practices in place at the neurological tissue banks, the left cerebral hemisphere was progressively frozen and stored at -80°C (post-mortem interval: 6–8 h). Therefore, the OB assessed in this study was the left one. The diagnosis was carried out on the right cerebral hemisphere. Following fixation in 10% formaldehyde for approximately three weeks, the brain was sectioned according to the recommendation guide proposed by BrainNet Europe [31]. After a macroscopic study, immunohistochemistry analysis was performed in different brain regions using specific antibodies against Tau protein, β amyloid, TDP-43, PrP, α -synuclein, ubiquitin and α - β crystalline. This brain did not show significant pathology and was considered to be healthy. In particular, the immunohistochemical study of the OB showed normal tissue without appreciable abnormalities.

2.2. Sample preparation for proteomic analysis

OB specimen was homogenized in lysis buffer containing 7 M urea, 2 M thiourea, 4% (v/v) CHAPS and 50 mM DTT. The homogenate was spun down at 100,000 $\times g$ for 1 h at 15°C . Protein concentration was measured in the supernatant with the Bradford assay kit (Biorad).

2.3. One-dimensional SDS-PAGE and in gel-trypsin digestion

Sample volume corresponding to 50 μg of human OB proteins were resuspended in loading buffer (7 M urea, 2 M thiourea, 4% (v/v) CHAPS, 50 mM DTT, 2% SDS, 0.1 M Tris pH 6.8, 30% glycerol and a trace of bromophenol blue) and applied on a 12% SDS-PAGE gel for 1 h at 120 V. After staining by colloidal coomassie (Invitrogen), gel image was acquired using GS800 densitometer (Biorad). Then, the gel lane was cut into 12 consecutive pieces and subjected to in-gel tryptic digestion. Briefly, gel pieces were destained and washed, and, after DTT reduction and iodoacetamide alkylation, the proteins were digested with porcine trypsin (modified sequence grade; Promega) in 50 mM ammonium bicarbonate overnight at 37°C . The resulting tryptic peptides were extracted with 5% formic acid, 50% acetonitrile. After digestion, the peptides obtained from each gel slice were analyzed using LC-MS/MS.

2.4. LC-MS/MS analysis using a Q-TOF instrument

Microcapillary reversed phase LC was performed with a nanoACQUITY UPLC system (Waters). Reversed phase separation of tryptic digests was performed with an Atlantis, C₁₈, 3 μm , 75 μm \times 10 cm Nano Ease™ fused silica capillary column (Waters) equilibrated in 5% acetonitrile, 0.2% formic acid. After injection of 6 μl of trypsinized sample originated from gel slide, the column was washed during 5 min with the same buffer and the peptides were eluted using a linear gradient of 5–50% acetonitrile in 30 min at a constant flow rate of 0.2 $\mu\text{l}/\text{min}$. The column was coupled online to a Q-TOF Micro (Waters) using a PicoTip nanospray ionization source (Waters). The heated capillary temperature was 80°C and the spray voltage was 1.8–2.2 kV. MS/MS data were collected in an automated data-dependent mode. The three most intense ions in each survey scan were sequentially fragmented by collision induced dissociation (CID) using an isolation width of 2.5 and a relative

collision energy of 35%. Data processing was performed with Masslynx 4.0. Database searching was done with Phenix 2.2 (GeneBio, Geneva, Switzerland) against Uniprot Knowledge-Base Release 15.14 consisting of UniprotKB/Swiss-Prot Release 57.14 and UniprotKB/TrEMBL Release 40.14 with 514,789 and 10,376,872 entries respectively. The search was enzymatically constrained for trypsin and allowed for one missed cleavage site. The parent ion error tolerances were 50 ppm and 800 ppm in MS and MS/MS mode respectively. Further search parameters were as follows: no restriction on molecular weight and isoelectric point; fixed modification, carbamidomethylation of cysteine; variable modification and oxidation of methionine.

2.5. Peptide fractionation

Protein material was precipitated using methanol/chloroform extraction. The pellet was dissolved in 100 mM Tris, pH 7.8, 6 M urea. Reduction was performed by addition of DTT to a final concentration of 10 mM and incubation at 25 °C for 1 h. Subsequent alkylation by 30 mM iodoacetamide was performed for 1 h in the dark. An additional reduction step was performed by 30 mM DTT, allowing the reaction to stand at 25 °C for 1 h. The solution was diluted to 0.6 M urea using MilliQ-water, and after trypsin addition (Promega) (enzyme:protein, 1:50, w/w), the sample was incubated at 37 °C for 18 h. The digestion mixture (~250 µg protein) was dried in a SpeedVac, reconstituted with 40 µl of 5 mM ammonium bicarbonate (ABC) pH 9.8, and injected to an Ettan LC system with a high pH stable X-Terra RP18 column (C18; 2.1 mm × 150 mm; 3.5 µm) (Waters) at a flow rate of 40 µl/min. Peptides were eluted with a mobile phase B of 5–65% linear gradient over 35 min (A, 5 mM ABC in water at pH 9.8; B, 5 mM ABC in acetonitrile at pH 9.8). Fourteen fractions were collected (see Supplementary Fig. 1), evaporated under vacuum and reconstituted into 15 µl of 2% acetonitrile, 0.1% formic acid and 98% water.

2.6. LC-MS/MS analysis using a Q-TRAP instrument

For each fraction, a total volume of 5 µl of tryptic peptides was injected with a flow rate of 250 nl/min in a nanoLC Ultra1D plus (Eksigent). A trap column Acclaim PepMap100 (100 µm × 2 cm; C18, 5 µm, 100 Å) and an analytical column Acclaim PepMap RSLC (75 µm × 15 cm, C18, 2 µm, 100 Å) from Dionex were used following the next gradient: 0–1 min (2% Buffer B), 1–110 min (2–30% Buffer B), 110–120 min (30–40% Buffer B), 120–125 min (40–90% Buffer B), 125–130 min (90% Buffer B), 130–132 min (90–2% Buffer B) and 132–150 min (2% Buffer B) (Buffer B (100% acetonitrile, 0.1% formic acid), Buffer A (0.1% formic acid)). MS analysis was performed on a Q-TRAP 5500 system (ABSciex) with a NanoSpray® III ion source (ABSciex) using Rolling Collision Energy in positive mode. Each fraction was analyzed twice in technical replicates. MS/MS data acquisition was performed using Analyst 1.5.2 (AB Sciex) and submitted to Protein Pilot™ Software (v.4.0.8085-ABSciex) using Paragon™ Algorithm [32] (v.4.0.0.0) for database search restricted to *Homo sapiens* (Database: uniprot_sprot_20100622; Unused ProtScore conf >0.05). False discovery rate was performed using a non lineal fitting method [33] and displayed results were those reporting a 5% global false discovery rate or better.

2.7. Data handling and bioinformatic analysis

The proteins identified in this study were classified by GOFact (<http://61.50.138.118/gofact>) (GOA version: gene_association.goa_human.72.20111115; protein/gene ID version: v3.87; 341222 entries for 41006 human proteins), where proteins are assigned in gene ontology (GO) terms, which rely on a controlled vocabulary for describing a protein in terms of its molecular function, biological process, or subcellular localization [34]. Reactome Database was used to analyze the distribution of human olfactory bulb proteins across specific reactions and biological pathways (<http://www.reactome.org>) [35]. The hydrophobicity property of plasma membrane proteins (GRAVY Index) was calculated using the ProtParam tool at ExPasy server (<http://web.expasy.org/protparam/>). Human orthologs and ID conversions were obtained using g:profiler (<http://biit.cs.ut.ee/gprofiler/gconvert.cgi>) and Protein Identifier Cross-Reference tool (PICR) (<http://www.ebi.ac.uk/Tools/picr/>) respectively.

3. Results

3.1. Identification of human olfactory bulb proteins by protein and peptide separation strategies coupled to LC-MS/MS

In the present study, we have used an autopsy specimen of the left OB from a human brain with the final goal to obtain a profound insight into the protein content and protein function of the OB. To reduce protein complexity, we used an integrated experimental workflow combining gel and chromatographic-based methods coupled to mass spectrometry (Fig. 1). First, proteins were separated by 1-DE and the stained gel was sliced in 12 portions followed by in-gel trypsin digestion. Using this protein fractionation approach, 236 proteins were unambiguously identified with ≥2 peptides in 12 LC-MS/MS runs (see Supplementary information). The second approach involved in-solution digestion followed by off-line RP-LC at basic pH to separate the peptide mixture. Replicate mass spectrometry measurements were performed in 14 peptide fractions, identifying 1259 protein species based on one peptide (237 proteins common in both replicates) and 1509 protein species with at least two peptides, where, more than 900 proteins were detected in both replicates (60% overlap) (See Supplementary Files 1 and 2 and Supplementary Fig. 2). Combining both approaches, we successfully identified 1529 protein species with a minimum of two peptides, corresponding to 1466 unique OB proteins.

Protein identification data from the current study were compared with previously published datasets of different components of olfactory system derived from large-scale proteomic studies. Specifically, we further compared the human OB proteins reported here to those of translational models such as rat and zebrafish OB, [29,30] membrane fraction from murine olfactory sensory cilia, [26,27] and human cleft mucus, [28] showing a 95%, 66%, 50%, and 68% overlapping respectively (Fig. 2).

3.2. Human olfactory bulb proteome characterization

A physicochemical characterization based on isoelectric point (pI) and molecular weight was performed in the OB protein

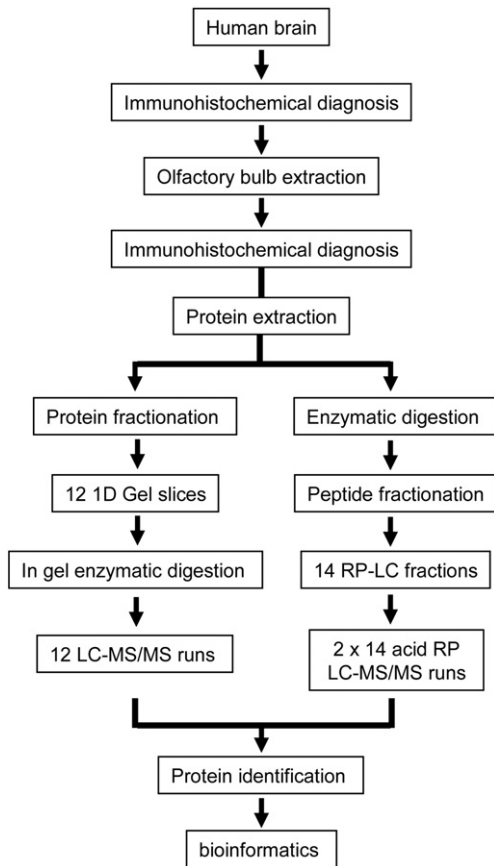


Fig. 1 – An overview of the procedure used for identification of the olfactory bulb proteome.

list. 56% of the identified proteins had a molecular weight lower than 50 kDa and 14.5% presented a mass > 100 kDa. The identified proteins were distributed across a wide pI range from 3.93 to 12.15. 16.7% of these proteins had pI > 9 and 13% presented pI values below 5. The pI and molecular weight distribution patterns for the identified proteins were compared with distribution patterns for the entire human proteome present in the International Protein Index (IPI) human database (Supplementary Fig. 3). It appears that our coverage is slightly biased toward the identification of proteins with pI 5–6. However, the region predicted to be rich in membrane associated proteins (pI > 8) is underrepresented compared to the whole proteome, presumably due to the better solubility and hence detection of cytosolic proteins compared to membrane proteins. Although proteins in the 25–50 kDa range were the most prevalent in the OB dataset, we identified a lower than expected proportion of proteins under 25 kDa compared to entire human proteome, probably due to the higher content of truncated forms of proteins, and bioactive peptides with small molecular weight in the human protein database (Supplementary Fig. 3).

To extract biological knowledge, OB proteome dataset was functionally categorized based on gene ontology (GO) annotation code [34] using the GOfact application, previously used by Human Liver Proteome Project (HLPP) [36]. From our dataset, 1425 identifiers were considered for further analysis.

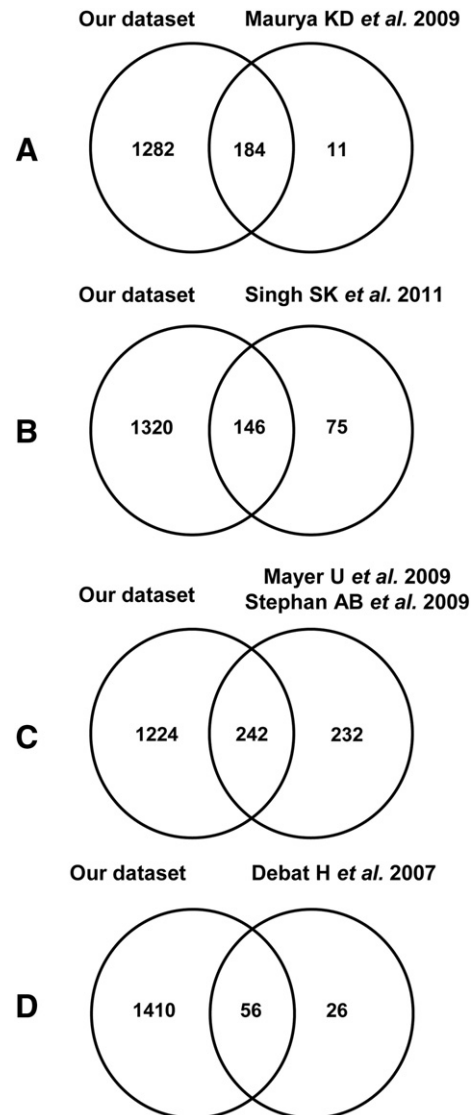


Fig. 2 – Venn diagrams of proteins found in olfactory system proteome datasets. Numbers represent the number of shared proteins in the respective overlapping areas. A) Rat proteins reported in OB [30]. B) Zebrafish (*Danio rerio*) proteins reported in OB [29]. C) Human olfactory proteins were compared against the combined rat and mouse olfactory sensory cilia (OSC) [26,27]. D) Human proteins reported in cleft mucus [28].

1348 (94.6%), 1281 (89.9%), and 1254 (88%) proteins were linked to at least one annotation term within the GO cellular component, biological process, and molecular function categories respectively. As shown in Fig. 3, 58% was accounted for cytosolic proteins. Another significant proportion of the identified proteins consisted of nuclear (30.6%), plasma membrane (23.5%), mitochondrial (21%), cytoskeletal (17%), and cytoplasmic vesicle (10.7%) proteins (Fig. 3). GO hierarchy also showed that 14% of OB identified proteins was associated to Golgi apparatus and endoplasmic reticulum. 5.5% of identified proteins correspond to the unknown group that cannot be found in the location information of GO database.

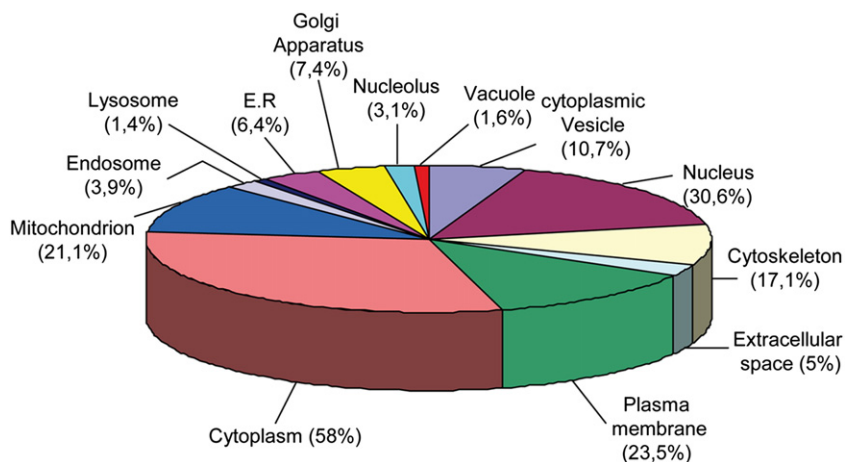


Fig. 3 – Gene ontology classification of olfactory bulb proteome based on cellular localization.

The remaining assignments included proteins present in the extracellular space (5%), endosome (3.9%), and nucleolus (3.1%) between others (Fig. 3). The Grand Average of Hydrophobicity Index (GRAVY index) was calculated for the 317 proteins annotated as plasma membrane proteins. The GRAVY values varied from -1.692 to 0.689 where 24 proteins (7.5%) had positive values (hydrophobic proteins).

With respect to the biological process category, 54 out of 69 GO terms were significantly enriched and 2 GO terms were significantly depleted compared with the entire list of IPI human database entries (see Supplementary Table 1 and Supplementary File 3). Only significantly enriched terms with a p -value $< 10^{-6}$ are represented in Fig. 4. These over-represented terms were mainly categorized in 7 groups (Fig. 4): metabolism (catabolism: 323 proteins; biosynthetic process: 235 proteins; macromolecule metabolism: 446 proteins; cellular metabolism: 750 proteins; generation of precursor metabolites: 115 proteins), cellular process (organelle organization: 204 proteins; cytoskeleton organization: 108 proteins; cell cycle: 86 proteins; signal transduction: 287 proteins; cell death: 108 proteins), cellular component organization (416 proteins), response to stimulus (response to stress: 208 proteins; response to endogenous stimulus: 84 proteins), establishment of localization (431 proteins), transport (427 proteins), and biological regulation (728 proteins) (Supplementary File 3).

With respect to the molecular function ontologies, 24 and 8 GO terms were significantly enriched and depleted respectively in human OB with respect to IPI entries (Supplementary Table 2 and Supplementary File 3). Over-represented categories can be divided in three main categories (Fig. 5). The first category included OB proteins with catalytic activity with an important enrichment of hydrolases (318 proteins), and phosphatases (pyrophosphatase activity: 177 proteins; nucleoside triphosphate activity: 171 proteins). The second category covered proteins involved in binding of different type of molecules such as RNA (101 proteins), nucleotide (404 proteins), protein (721 proteins), and receptor (103 proteins). The third category includes electron carrier activity (41 proteins). Under-represented terms mainly included DNA binding (85 proteins), transcription regulator activity (30 proteins), and

signal transducer activity (54 proteins) between others (Supplementary File 3).

3.3. Contribution to the repertoire of human brain proteome

The human OB proteome dataset was also compared with previously published lists of human brain proteome descriptions. Of the 1832 non-redundant proteins identified by HBPP studies [37–39], 835 have been recovered in our analysis. Interestingly, 631 novel proteins were identified in human OB with median sequence coverage of 24% (Fig. 6A). We performed a detailed analysis of peptide coverage in this dataset. 301 out of 631 proteins (48%) were identified with two or more peptides in both replicates. In particular, 240 and 93 proteins were identified with two or three peptides respectively in replicate 1. On the other hand, 167 and 103 proteins were detected with two or three peptides in replicate 2 (Supplementary Fig. 4). Although some specific OB proteins have been identified in OB such as olfactory marker protein, these data indicate that a considerable proportion of this protein list was identified with a low number of peptides suggesting that the discovery of this subset of proteins in the olfactory bulb may be due to technical bias rather than specific enrichment of these proteins in the OB with respect to other brain regions.

We have analyzed the HBPP proteome dataset with the latest release of the IPI database (v3.87) using GOfact tool to provide an updated functional view of the dataset circumventing the fluctuations in genome annotations and to make OB and brain protein lists comparable from a functional point of view (see Supplementary File 4). In particular, a comparative functional analysis between proteins exclusively identified in human OB and HBPP studies (631 and 997 proteins respectively) was performed in order to eliminate potential noise derived from the global comparison of both complete datasets (Fig. 6B and Supplementary File 5). From 631 OB identifiers, 604 were considered for further analysis. 527 (87.3%), 559 (92.5%), and 509 (84.3%) proteins were linked to at least one annotation term within GO biological process, cellular component, and molecular function respectively.

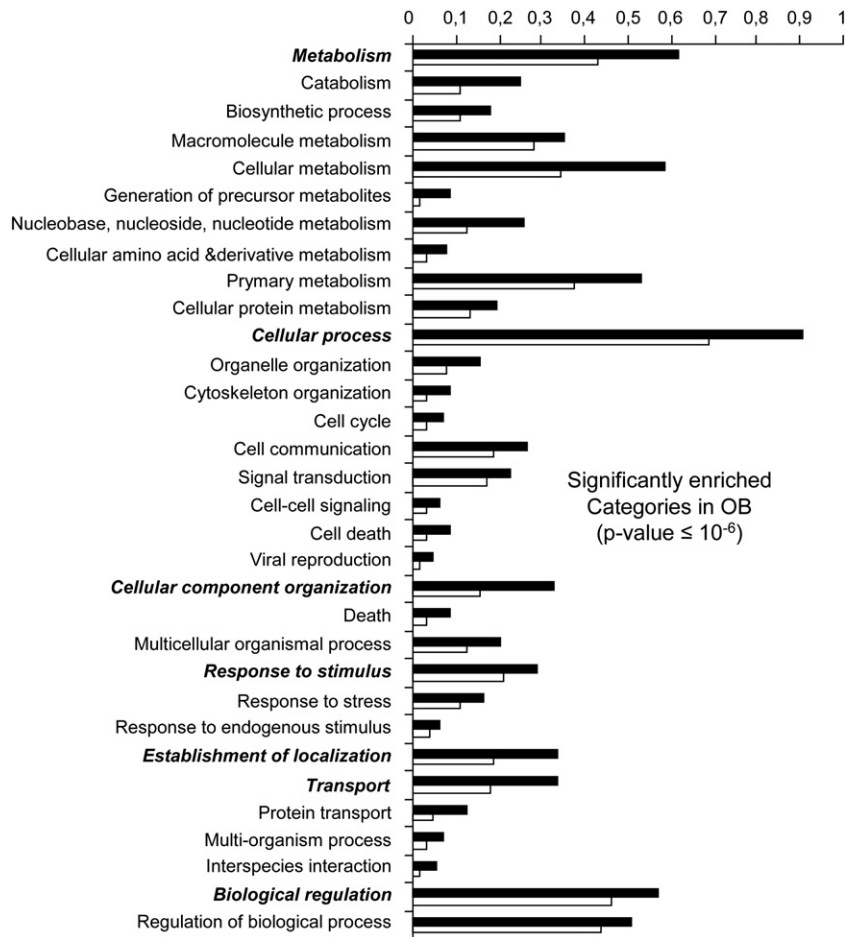


Fig. 4 – Significantly enriched GO biological process terms for the OB proteomic expression profile ($p < 1 \times 10^{-6}$). The ratio shown is the number of OB proteins and entire IPI proteins annotated to each GO term divided by the number of OB proteins and entire IPI proteins linked to at least one annotation term in the GO biological process categories. (See Supplementary Table 1). Black and white bars correspond to OB proteome dataset and entire IPI human database respectively.

With respect to 997 proteins derived from HBPP studies, 684 identifiers (68.3%) were considered for GO analysis (biological process: 546 proteins (79.8%); cellular component: 580 proteins (84.8%); molecular function: 528 proteins (77.2%)). As shown in Fig. 6B, GO terms corresponding to ribonucleoprotein complex, nucleus, extracellular space, and vacuole were significantly enriched in human OB and no significant over-representation was detected in human brain with respect to the entire IPI database. On the other hand, terms associated with microsomal fraction such as membrane and Golgi apparatus were significantly enriched in human brain. With respect to biological process categories, GO terms corresponding to different aspects of regulation of metabolic process and response to stimulus were slightly overrepresented in OB whereas terms related to cell recognition and adhesion were enriched in HBPP data (Fig. 6B). With respect to molecular function ontologies, GO terms related to hydrolase and phosphatase activities were significantly over-represented in OB dataset while other GO terms such as kinase and different binding activities were significantly enriched in HBPP dataset with respect to OB dataset (Fig. 6B). Due to the high functional parallelism observed between OB and brain proteome

descriptions with respect to cell component, biological process, and molecular function categories (see Supplementary Files 3 and 4), subsequent analyses were performed to analyze the differential OB protein dataset distribution across specific biological reactions using Reactome Database [35]. 310 out of 631 OB proteins were mapped to 365 biological reactions (Supplementary File 6) being proteasome mediated degradation, gene expression, metabolism and hemostasis the general over-represented processes. Interestingly, as shown in Table 1, some statistically over-represented processes were directly relevant to electrical machinery and synaptic plasticity.

4. Discussion

The OB is the first site for the processing of odor information in the brain and its dysfunction is known to be among the earliest preclinical signs of Alzheimer's and Parkinson's diseases [40]. It is important to note that most of human OB samples available in Neurological Tissue Banks derived from patients with advanced stages of Parkinson and Alzheimer

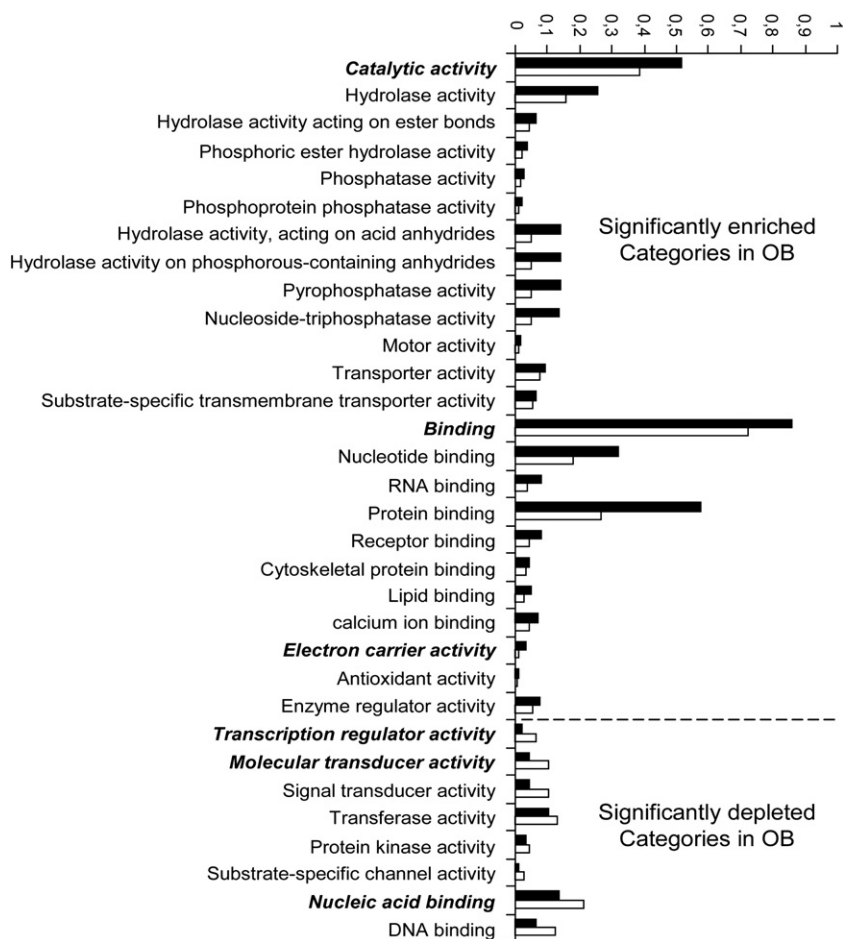


Fig. 5 – Significantly enriched and depleted GO molecular function terms for the OB proteomic expression profile ($p < 0.05$). The ratio shown was calculated as described in the legend of Fig. 4 (See Supplementary Table 2). Black and white bars correspond to OB dataset and entire IPI human database respectively.

diseases that have been subjected to a diverse variety of pharmacological treatments. This aspect is crucial because there is a very limited availability of healthy OB samples, which hamper the development of quantitative proteomic analysis of control and pathological-OB samples to discover new targets, and develop novel diagnostic strategies in neurodegenerative diseases.

Due to its relevance in a broad-spectrum of neurological disorders, [14,40,41] we have performed an in-depth analysis of the protein content of a well-characterized healthy human OB using protein and peptide fractionation methods coupled to tandem mass spectrometry. Similar experimental workflows have been successfully applied in proteome characterization of different human body fluids [42,43] and also in human tissues such as brain [37]. In the peptide fractionation approach, we have obtained a 60% overlap in analytical replicates in terms of protein identification, probably due to the “missing value problem” caused by the semi-random nature of peak selection for fragmentation [44]. Encompassing the 40 LC-MS/MS runs performed in both separative approaches, a non-redundant set of 1466 unique proteins were identified with median sequence coverage of 34%. This protein dataset increases significantly the catalog of proteins identified in the olfactory system so far, [26–30] revealing 631

proteins not previously described before in the HBPP studies [37–39]. A considerable proportion of these differential proteins have been identified with 2 or 3 peptides, indicating that the identification may be probably due to a technical origin rather than a biological enrichment of these proteins in the OB. However, some proteins involved in cytoskeletal rearrangement have been exclusively identified in OB. Cytoplasmic dynein 1 heavy chain, AHNAK/desmoyokin, spectrin beta chain, and microtubule-associated protein 1B have been identified with more than 30 peptides in both replicates and Plectin-1 and brain spectrin alpha chain with more than 130 peptides also in both replicates. These large proteins, not identified in HBPP studies, may participate in the neurite extension and cell differentiation process that occurs in the OB. In agreement with intracellular distribution of proteins in human brain, [45] most of the proteins identified in OB are cytoplasmic with a clear enrichment of nuclear and mitochondrial proteins, proteins associated to cytoskeleton, and cytoplasmic-membrane bound vesicle components. Similar subcellular distribution has been also described in human skeletal muscle proteome, [46] in contrast with the distribution observed in proteomic studies derived from metabolic tissues such as the heart and the liver where most of the assignments are directly related to organelles [36,47,48]. With

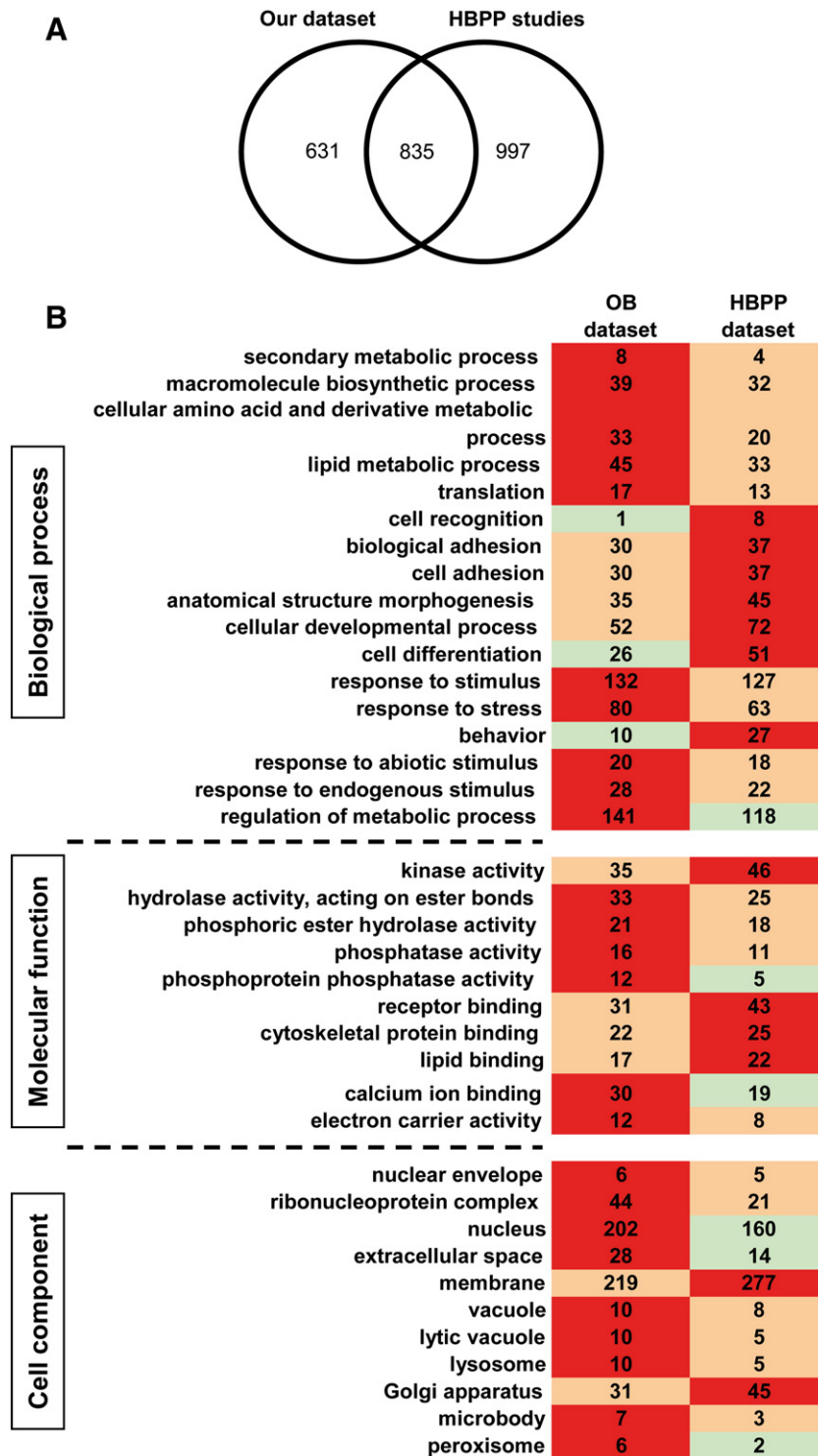


Fig. 6 – Comparison with human brain proteome dataset. A) Venn diagram showing the overlap between our study (left circle) and the total number of human brain proteins identified in large-scale proteomic studies up to now (right circle). B) Functional comparative analysis between unique HBPP and OB protein datasets. Both datasets were processed independently by GOfact and statistically significant enriched and depleted differential GO terms are shown. Numbers inside the boxes represent the number of proteins assigned in each GO category. Color code: light red (enriched), light green (depleted), red (significantly enriched with respect to entire IPI human database) and green (significantly depleted with respect to entire IPI human database).

Table 1 – Over-representation of OB proteins in specific-neuronal processes by Reactome pathway analysis. p-value indicates the probability of detect OB proteins in each event by chance. See Supplementary File 6 to show the specific proteins in each event.

Name of the event	Proteins in this event	Total no. of proteins	p-value
Axon guidance	37	281	8.4e-08
Dephosphorylation/autophosphorylation of NCAM1 bound pFyn	6	10	3.2e-06
Glutamate binding, activation of AMPA receptors and synaptic plasticity	8	30	9.9e-05
Trafficking of AMPA receptors	8	30	9.9e-05
Opioid signaling	13	80	2.0e-04
NCAM signaling for neurite out-growth	11	70	8.1e-04
Axonal transport of NGF: Trk complexes	4	11	1.7e-03
Neurotransmitter receptor binding. Transmission in the postsynaptic cell	15	136	4.1e-03
Retrograde neurotrophin signaling	4	14	4.6e-03
Signaling by Robo receptor	6	32	5.2e-03
Trafficking of GluR2-containing AMPA receptors to extrasynaptic sites	4	15	6.0e-03
Synapsis, or interaction between two DNA-PK: DNA complexes	2	3	7.7e-03
Transmission across chemical synapses	18	189	8.4e-03
NGF signaling via TRKA from the plasma membrane	14	136	1.0e-02
NrCAM binds synapse-associated proteins	2	4	1.5e-02
XRCC4: DNA ligase IV complex with the DNA-PK: DNA synaptic complex	2	5	2.4e-02
BoNT light chain types B, D, and F cleave VAMP/synaptobrevin	2	5	2.4e-02
Sema3A PAK dependent axon repulsion	3	15	3.9e-02
Plexin-A binds to neuropilin-1	2	7	4.7e-02

respect to OB plasma membrane proteins, 30% has been previously localized in the membrane cilia of olfactory sensory neurons [26,27]. With regard to molecular function categories, a specific enrichment of catalytic and binding activities was detected in human OB with respect to the entire IPI database. In particular, nucleoside triphosphatase, nucleotide, and RNA binding activities were well-represented in the dataset with 171, 404, and 101 proteins respectively. Eight different subunits (A, B, C1, D, d1, E1, F, H) of the vacuolar proton-pumping ATPase have been identified in OB proteome analysis. This V-type ATPase plays a role in acidifying the mucous layer, which is important to mediate the sensitivity to odorants in the olfactory epithelium where four subunits of this complex enzyme present a cell type specific localization [49]. Additionally, all isoforms of plasma membrane calcium-transporting ATPase have been detected in our proteomic study. These calcium pumps are present in OSN [50] and participate in the clearance of accumulated calcium within the olfactory cilia during the odor response [51,52]. In accordance with HBPP studies, [45] a high number of GTPases have been also identified in OB such as 19 Rab GTPases, 6 Arf GTPases, and 5 dynamins. These families of proteins are membrane trafficking regulators present in synaptic vesicles, acting in vesicle biogenesis, [53] vesicle connection, [54] and olfactory cilium formation, [55] and some of them have been previously localized in murine OB [24,56]. Although a significant under-representation of transcription regulator and nucleic acid binding activities was common between human OB and brain proteomes, [45] a specific enrichment of proteins with RNA binding activities was detected in both tissues. In particular, 20% of the identified OB RNA-binding proteins correspond to heterogeneous nuclear ribonucleoproteins (HnRNPs) involved in RNA trafficking, stability and translation. These proteins bind to A2RE-containing neuronal RNAs that move along dendrites in response to synaptic activities related to memory formation [57]. Specifically, an impairment

of nNOS leads to a deregulation of olfactory long term memory consolidation, altering some HnRNP protein levels in mouse OB [58]. Another important protein identified was the olfactory marker protein, a modulator of the olfactory signal-transduction cascade [59] critical for functional maturation of OSNs [60].

Although a comprehensive functional annotation of the human brain proteome has been previously characterized, [45] we have considered necessary to re-analyze HBPP and OB data with the same updated database to get a comparable functional outcome. In spite of 631 additional proteins identified in human OB were not previously reported in HBPP studies, only some significant differences have been detected in some broad and overlapping GO terms indicating that OB dataset increases the number of proteins assigned in the majority of GO terms with respect to HBPP studies but without substantially modifying the integrated functional interpretation. However, based on manually curated and peer-reviewed biological pathways from Reactome Database, [35] we have obtained a deeper functional analysis of the differential OB protein dataset. Based on Reactome analysis, specific isoforms of spectrin (spectrin alpha erythrocytic 1, spectrin alpha non erythrocytic 1, spectrin beta chain brain and erythrocyte isoforms, spectrin beta non erythrocytic 1), GTPase KRas, and tyrosine protein kinase Fyn are interactors of neural cell adhesion molecule 1 (NCAM1), a crucial protein in the formation of OB as derived from studies in NCAM1-knock-out mice [61]. In particular, this cluster of proteins participate in the signaling pathway of NCAM-dependent neurite outgrowth, [62–64] preventing uncontrolled elongation of neuronal processes. Reactome pathway analysis also pointed out that signaling mediators such as AP-2 complex subunits alpha, beta, and mu, PP2A catalytic subunit alpha-isoform, and calcium/calmodulin dependent protein kinase IV between others, are related to nerve growth factor (NGF)/TRKA signaling. Apart of regulating neuronal survival, axonal

growth, and synaptic plasticity, [65] this pathway plays an essential role in the development, maintenance, and regeneration of olfactory receptor cells [66].

5. Conclusions

Taken together, our results provide a broad functional analysis of 1466 non-redundant human OB proteins, being the first step toward the complete characterization of this brain subproteome. Due to that OB is anatomically well-demarcated area with different spatial patterns of gene expression, [67] the development of specific isolation and purification protocols of single-cell types from OB, [68,69] together with novel developments in shotgun proteomic approaches, [70] would allow to explore the transcriptome and proteome profiling of each olfactory cell population individually, [71] increasing the molecular knowledge of the OB.

Acknowledgments

We thank the Neurological Tissue Bank of Navarra Health Service for providing us the OB specimen. We are grateful to Ana Aramendía and Carmen Echávarri from the Neurological Tissue Bank of Navarra Health Service for immunohistochemical analysis and for sharing experiences on human brain processing. The technical assistance of María I. Mora from Proteomics Core Facility at CIMA is highly appreciated. We also thank Christian Stephan and Helmut E. Meyer from Medizinisches Proteom-Center at Ruhr-University Bochum for providing us the unified protein dataset derived from HBPP proteomic studies and for critical evaluation of the manuscript. This work was supported by Miguel Servet Foundation (Government of Navarra) and the agreement between FIMA and the “UTE project CIMA”. Grant Plan Nacional I+D+I SAF2008-0154 from Ministerio de Ciencia e Innovación to FJC. The Proteomics Core Facility at CIMA is a member of the National Institute of Proteomics Facilities, ProteoRed.

Appendix A. Supplementary data

Supplementary data to this article can be found online at <http://dx.doi.org/10.1016/j.jprot.2012.05.011>.

REFERENCES

- Firestein S. How the olfactory system makes sense of scents. *Nature* 2001;413:211–8.
- Buck L, Axel R. A novel multigene family may encode odorant receptors: a molecular basis for odor recognition. *Cell* 1991;65:175–87.
- Zhang X, Firestein S. Comparative genomics of odorant and pheromone receptor genes in rodents. *Genomics* 2007;89:441–50.
- Maresh A, Rodriguez Gil D, Whitman MC, Greer CA. Principles of glomerular organization in the human olfactory bulb—implications for odor processing. *PLoS One* 2008;3:e2640.
- Mori K, Nagao H, Yoshihara Y. The olfactory bulb: coding and processing of odor molecule information. *Science* 1999;286:711–5.
- Whitman MC, Greer CA. Adult neurogenesis and the olfactory system. *Prog Neurobiol* 2009;89:162–75.
- Lewin B. On neuronal specificity and the molecular basis of perception. *Cell* 1994;79:935–43.
- Carleton A, Petreanu LT, Lansford R, Alvarez-Buylla A, Lledo PM. Becoming a new neuron in the adult olfactory bulb. *Nat Neurosci* 2003;6:507–18.
- Gould E, Reeves AJ, Graziano MS, Gross CG. Neurogenesis in the neocortex of adult primates. *Science* 1999;286:548–52.
- Gheusi G, Cremer H, McLean H, Chazal G, Vincent JD, Lledo PM. Importance of newly generated neurons in the adult olfactory bulb for odor discrimination. *Proc Natl Acad Sci U S A* 2000;97:1823–8.
- Curtis MA, Faull RL, Eriksson PS. The effect of neurodegenerative diseases on the subventricular zone. *Nat Rev Neurosci* 2007;8:712–23.
- Meisami E, Mikhail L, Baim D, Bhatnagar KP. Human olfactory bulb: aging of glomeruli and mitral cells and a search for the accessory olfactory bulb. *Ann N Y Acad Sci* 1998;855:708–15.
- Bhatnagar KP, Kennedy RC, Baron G, Greenberg RA. Number of mitral cells and the bulb volume in the aging human olfactory bulb: a quantitative morphological study. *Anat Rec* 1987;218:73–87.
- Turetsky BI, Moberg PJ, Arnold SE, Doty RL, Gur RE. Low olfactory bulb volume in first-degree relatives of patients with schizophrenia. *Am J Psychiatry* 2003;160:703–8.
- Fusari A, Molina JA. Sense of smell, physiological ageing and neurodegenerative diseases: II. Ageing and neurodegenerative diseases. *Rev Neurol* 2009;49:363–9.
- Zivadinov R, Zorzon M, Monti Bragadin L, Pagliaro G, Cazzato G. Olfactory loss in multiple sclerosis. *J Neurol Sci* 1999;168:127–30.
- Strous RD, Shoenfeld Y. To smell the immune system: olfaction, autoimmunity and brain involvement. *Autoimmun Rev* 2006;6:54–60.
- Olichney JM, Murphy C, Hofstetter CR, Foster K, Hansen LA, Thal LJ, et al. Anosmia is very common in the Lewy body variant of Alzheimer’s disease. *J Neurol Neurosurg Psychiatry* 2005;76:1342–7.
- McShane RH, Nagy Z, Esiri MM, King E, Joachim C, Sullivan N, et al. Anosmia in dementia is associated with Lewy bodies rather than Alzheimer’s pathology. *J Neurol Neurosurg Psychiatry* 2001;70:739–43.
- Bayes A, Grant SG. Neuroproteomics: understanding the molecular organization and complexity of the brain. *Nat Rev Neurosci* 2009;10:635–46.
- Liao L, McClatchy DB, Yates JR. Shotgun proteomics in neuroscience. *Neuron* 2009;63:12–26.
- Vaishnav RA, Getchell ML, Poon HF, Barnett KR, Hunter SA, Pierce WM, et al. Oxidative stress in the aging murine olfactory bulb: redox proteomics and cellular localization. *J Neurosci Res* 2007;85:373–85.
- Murrey HE, Ficarro SB, Krishnamurthy C, Domino SE, Peters EC, Hsieh-Wilson LC. Identification of the plasticity-relevant fucose-alpha(1-2)-galactose proteome from the mouse olfactory bulb. *Biochemistry* 2009;48:7261–70.
- Poon HF, Vaishnav RA, Butterfield DA, Getchell ML, Getchell TV. Proteomic identification of differentially expressed proteins in the aging murine olfactory system and transcriptional analysis of the associated genes. *J Neurochem* 2005;94:380–92.
- Li L, Mauric V, Zheng JF, Kang SU, Patil S, Hoger H, et al. Olfactory bulb proteins linked to olfactory memory in C57BL/6j mice. *Amino Acids* 2010;39:871–86.
- Mayer U, Kuller A, Daiber PC, Neudorf I, Warnken U, Schnolzer M, et al. The proteome of rat olfactory sensory cilia. *Proteomics* 2009;9:322–34.

- [27] Stephan AB, Shum EY, Hirsh S, Cygnar KD, Reiser J, Zhao H. ANO2 is the cilia calcium-activated chloride channel that may mediate olfactory amplification. *Proc Natl Acad Sci U S A* 2009;106:11776–81.
- [28] Debat H, Eloit C, Blon F, Sarazin B, Henry C, Huet JC, et al. Identification of human olfactory cleft mucus proteins using proteomic analysis. *J Proteome Res* 2007;6:1985–96.
- [29] Singh SK, Saxena S, Meena Lakshmi MG, Saxena P, Idris MM. Proteome Profile of Zebrafish *Danio rerio* Olfactory Bulb Based on Two-Dimensional Gel Electrophoresis Matrix-Assisted Laser Desorption/Ionization MS/MS Analysis. *Zebrafish* 2011;8:183–9.
- [30] Maurya DK, Sundaram CS, Bhargava P. Proteome profile of the mature rat olfactory bulb. *Proteomics* 2009;9:2593–9.
- [31] Bell JE, Alafuzoff I, Al-Sarraj S, Arzberger T, Bogdanovic N, Budka H, et al. Management of a twenty-first century brain bank: experience in the BrainNet Europe consortium. *Acta Neuropathol* 2008;115:497–507.
- [32] Shilov IV, Seymour SL, Patel AA, Loboda A, Tang WH, Keating SP, et al. The Paragon Algorithm, a next generation search engine that uses sequence temperature values and feature probabilities to identify peptides from tandem mass spectra. *Mol Cell Proteomics* 2007;6:1638–55.
- [33] Tang WH, Shilov IV, Seymour SL. Nonlinear fitting method for determining local false discovery rates from decoy database searches. *J Proteome Res* 2008;7:3661–7.
- [34] Ashburner M, Ball CA, Blake JA, Botstein D, Butler H, Cherry JM, et al. Gene ontology: tool for the unification of biology. *The Gene Ontology Consortium*. *Nat Genet* 2000;25:25–9.
- [35] Haw R, Hermjakob H, D'Eustachio P, Stein L. Reactome pathway analysis to enrich biological discovery in proteomics data sets. *Proteomics* 2011;11:3598–613.
- [36] Chen M, Ying W, Song Y, Liu X, Yang B, Wu S, et al. Analysis of human liver proteome using replicate shotgun strategy. *Proteomics* 2007;7:2479–88.
- [37] Park YM, Kim JY, Kwon KH, Lee SK, Kim YH, Kim SY, et al. Profiling human brain proteome by multi-dimensional separations coupled with MS. *Proteomics* 2006;6:4978–86.
- [38] Fröhlich T, Helmstetter D, Zobawa M, Crecelius AC, Arzberger T, Kretzschmar HA, et al. Analysis of the HUPRO Brain Proteome reference samples using 2-D DIGE and 2-D LC-MS/MS. *Proteomics* 2006;6:4950–66.
- [39] Hamacher M, Apweiler R, Arnold G, Becker A, Bluggel M, Carrette O, et al. HUPRO Brain Proteome Project: summary of the pilot phase and introduction of a comprehensive data reprocessing strategy. *Proteomics* 2006;6:4890–8.
- [40] Doty RL. The olfactory system and its disorders. *Semin Neurol* 2009;29:74–81.
- [41] Dode C, Hardelin JP. Kallmann syndrome: fibroblast growth factor signaling insufficiency? *J Mol Med* 2004;82:725–34.
- [42] Adachi J, Kumar C, Zhang Y, Olsen JV, Mann M. The human urinary proteome contains more than 1500 proteins, including a large proportion of membrane proteins. *Genome Biol* 2006;7:R80.
- [43] de Souza GA, Godoy LM, Mann M. Identification of 491 proteins in the tear fluid proteome reveals a large number of proteases and protease inhibitors. *Genome Biol* 2006;7:R72.
- [44] Nagaraj N, Kulak NA, Cox J, Neuhaus N, Mayr K, Hoerning O, et al. Systems-wide perturbation analysis with near complete coverage of the yeast proteome by single-shot UHPLC runs on a bench-top Orbitrap. *Mol Cell Proteomics*.
- [45] Mueller M, Martens L, Reidegeld KA, Hamacher M, Stephan C, Bluggel M, et al. Functional annotation of proteins identified in human brain during the HUPRO Brain Proteome Project pilot study. *Proteomics* 2006;6:5059–75.
- [46] Yi Z, Bowen BP, Hwang H, Jenkinson CP, Coletta DK, Lefort N, et al. Global relationship between the proteome and transcriptome of human skeletal muscle. *J Proteome Res* 2008;7:3230–41.
- [47] Ruse CI, Tan FL, Kinter M, Bond M. Integrated analysis of the human cardiac transcriptome, proteome and phosphoproteome. *Proteomics* 2004;4:1505–16.
- [48] Bousette N, Kislinger T, Fong V, Isserlin R, Hewel JA, Emil A, et al. Large-scale characterization and analysis of the murine cardiac proteome. *J Proteome Res* 2009;8:1887–901.
- [49] Paunescu TG, Jones AC, Tyszkowski R, Brown D. V-ATPase expression in the mouse olfactory epithelium. *Am J Physiol Cell Physiol* 2008;295:C923–30.
- [50] Weeraratne SD, Valentine M, Cusick M, Delay R, Van Houten JL. Plasma membrane calcium pumps in mouse olfactory sensory neurons. *Chem Senses* 2006;31:725–30.
- [51] Saidu SP, Weeraratne SD, Valentine M, Delay R, Van Houten JL. Role of plasma membrane calcium ATPases in calcium clearance from olfactory sensory neurons. *Chem Senses* 2009;34:349–58.
- [52] Kleene SJ. Limits of calcium clearance by plasma membrane calcium ATPase in olfactory cilia. *PLoS One* 2009;4:e5266.
- [53] Pasqualato S, Renault L, Cherfils J. Arf, Arl, Arp and Sar proteins: a family of GTP-binding proteins with a structural device for 'front-back' communication. *EMBO Rep* 2002;3:1035–41.
- [54] Schimmoller F, Simon I, Pfeffer SR. Rab GTPases, directors of vesicle docking. *J Biol Chem* 1998;273:22161–4.
- [55] Yoshimura S, Egerer J, Fuchs E, Haas AK, Barr FA. Functional dissection of Rab GTPases involved in primary cilium formation. *J Cell Biol* 2007;178:363–9.
- [56] Tavitian B, Moya KL, Doignon I, Stettler O. Differential effect of functional olfactory deprivation on synaptic vesicle proteins in rat olfactory bulb. *Neuroreport* 1995;6:1449–53.
- [57] Smith R. Moving molecules: mRNA trafficking in Mammalian oligodendrocytes and neurons. *Neuroscientist* 2004;10:495–500.
- [58] Juch M, Smalla KH, Kahne T, Lubec G, Tischmeyer W, Gundelfinger ED, et al. Congenital lack of nNOS impairs long-term social recognition memory and alters the olfactory bulb proteome. *Neurobiol Learn Mem* 2009;92:469–84.
- [59] Koo JH, Gill S, Pannell LK, Menco BP, Margolis JW, Margolis FL. The interaction of Bex and OMP reveals a dimer of OMP with a short half-life. *J Neurochem* 2004;90:102–16.
- [60] Lee AC, He J, Ma M. Olfactory marker protein is critical for functional maturation of olfactory sensory neurons and development of mother preference. *J Neurosci* 2011;31:2974–82.
- [61] Ronn LC, Hartz BP, Bock E. The neural cell adhesion molecule (NCAM) in development and plasticity of the nervous system. *Exp Gerontol* 1998;33:853–64.
- [62] Kolkova K, Novitskaya V, Pedersen N, Berezin V, Bock E. Neural cell adhesion molecule-stimulated neurite outgrowth depends on activation of protein kinase C and the Ras-mitogen-activated protein kinase pathway. *J Neurosci* 2000;20:2238–46.
- [63] Korshunova I, Novitskaya V, Kiryushko D, Pedersen N, Kolkova K, Kropotova E, et al. GAP-43 regulates NCAM-180-mediated neurite outgrowth. *J Neurochem* 2007;100:1599–612.
- [64] Ramser EM, Buck F, Schachner M, Tilling T. Binding of alphaII spectrin to 14–3–3beta is involved in NCAM-dependent neurite outgrowth. *Mol Cell Neurosci* 2010;45:66–74.
- [65] Lykissas MG, Batistatou AK, Charalabopoulos KA, Beris AE. The role of neurotrophins in axonal growth, guidance, and regeneration. *Curr Neurovasc Res* 2007;4:143–51.
- [66] Miwa T, Moriizumi T, Horikawa I, Uramoto N, Ishimaru T, Nishimura T, et al. Role of nerve growth factor in the olfactory system. *Microsc Res Tech* 2002;58:197–203.

- [67] Lin DM, Yang YH, Scolnick JA, Brunet LJ, Marsh H, Peng V, et al. Spatial patterns of gene expression in the olfactory bulb. *Proc Natl Acad Sci U S A* 2004;101:12718–23.
- [68] Pagano SF, Impagnatiello F, Girelli M, Cova L, Grioni E, Onofri M, et al. Isolation and characterization of neural stem cells from the adult human olfactory bulb. *Stem Cells* 2000;18:295–300.
- [69] Liu Y, Teng X, Yang X, Song Q, Lu R, Xiong J, et al. Shotgun proteomics and network analysis between plasma membrane and extracellular matrix proteins from rat olfactory ensheathing cells. *Cell Transplant* 2010;19:133–46.
- [70] Beck M, Schmidt A, Malmstroem J, Claassen M, Ori A, Szymborska A, et al. The quantitative proteome of a human cell line. *Mol Syst Biol* 2011;7:549.
- [71] Nagaraj N, Wisniewski JR, Geiger T, Cox J, Kircher M, Kelso J, et al. Deep proteome and transcriptome mapping of a human cancer cell line. *Mol Syst Biol* 2011;7:548.